The International Journal of Advanced Manufacturing Technology (2022) 121:2747–2757
https://doi.org/10.1007/s00170-022-09472-x

ORIGINAL ARTICLE

Avoiding feed fluctuation for five-axis interpolation using 3D clothoid and B-spline

Zheng Sun[1,2] · Liyong Niu[1] · Bin Liu[1,2] · Kedian Wang[1] · Bo Li[3] · Xuesong Mei[1]

Received: 3 November 2021 / Accepted: 31 May 2022 / Published online: 16 June 2022

Abstract
For the CNC machine tools, the feedrate fluctuation may excite the vibration of the machine structures and damage the surface of machined parts. This paper presents a novel interpolation solution for 5-axis machining to avoid feedrate fluctuation. The path of TCP is globally smoothed through the 3D clothoid, whose interpolation parameter is just the curve length. The path of tool orientation is fitting with the B-spline, which can reach any order of continuity under the requirement. The effectiveness of the proposed interpolation method is verified through the simulation and the experimental test on a 5-axis machine tool. Compared with the state-of-the-art, the proposed method attenuates the feedrate fluctuation with more order of magnitude.

Keywords Tool path smoothing · Curve fitting · Clothoid · Interpolation · CNC

1 Introduction

The tool path for a computer numerical controlled (CNC) machine tool is described through the G-code (ISO 6983). For the machining of a "free form" surface, the curve of the tool path generated by the computer-aided manufacturing (CAM) system can only be approximated through data-intensive piecewise line commands. The connecting between these pieces ensures the C^0-continuity only. Moving along with such an approximated curve, the vibration of the machine structure will be excited and the quality of machined parts is damaged, consequently.

In order to cover this gap, various smooth/fitting solutions for 5-axis machining have been proposed. From different aspects, these solutions can be divided as shown in Table 1.

From the aspect of tool pose representation, the tool path for 5-axis machining can be represented as a path combination of the tool center point (TCP) and the tool orientation (TO), or the combination of the TCP and the path of the second point on the tool axis (TA), as shown in Fig. 1. Both of them define the movement of TCP in the cartesian coordinate system as a curve approximated through piecewise segments, whose vertices (knots) are given by the G-code. For 5-axis machining, two additional angle values (A and C axes) are also given to describe the tool orientation at each knot. The TCP + TO representation interpolates the TO in the spherical coordinate system through NURBS or B-spline [6, 7, 15–17], PH-spline [8], etc. The TCP + TA representation calculates the knots of TA through the TCP coordinate and orientation given by the G-code firstly and then smooths the TA locally or globally in the cartesian coordinate system, as shown in Fig. 1, right. The distance between two interpolated points of each curve should always keep constant, normally the length of the tool. But this representation can only guarantee the constant distance between the corresponding knots of each curve if the global smooth strategy is used. To improve distance preservation, the compact dual NURBS [10] or the dual NURBS based on the quaternion [11] are constructed. For the local smooth strategy, the constraint of constant distance lacks sufficient investigation.

From the aspect of smooth strategy, these solutions can be divided into local smooth solutions and global smooth solutions, as shown in Fig. 2. The local solutions keep the main part of the approximated segments and connect two neighboring segments through a designed spline. Different from the local solutions, the global smooth represents all the segments as a curve with high-order continuity passing through all the given knots in the cartesian system (TCP, TA) or

✉ Bin Liu
liubin1110@xjtu.edu.cn

[1] State Key Laboratory for Manufacturing Systems Engineering, Xi'an Jiaotong University, Xi'an, China

[2] Suzhou Institute, Xi'an Jiaotong University, Xi'an, China

[3] CNBHC Co. Ltd, Chengdu, China

Table 1 Category of smooth solution

	Local smoothing	Global smoothing
TCP + TA	B-spline: [1, 2] NURBS: [3] Bézier: [4, 5]	NURBS: [9–11] B-spline: [12, 13]
TCP + TO	B-spline: [6, 7] PH-spline: [8]	Quintic + Bézier: [14] B-spline: [15–17]

the spherical system (TO). To synchronize the movement of two fitting curves, some scholars use a unique interpolation parameter [9, 10] or establish two interpolation parameters with a linear relationship [6]. However, it may lead to the large shaking of the tool orientation at some critical points with large curvature [11]. To solve this problem, nonlinear relationships are established, such as the reparameterization spline [14] or the polynomial with 9-order [15].

The most used spline for smoothing the curves are the quintic spline [18], Pythagorean-Hodograph (PH) spline [19], and NURBS/B-spline [13]. These splines have the good property of continuity and can be mathematically easily formulated. However, the length of these curves is not linearly matched to the interpolation parameter, which means the real increased curve length from the interpolation does not exactly equal the length planed by the motion control function. It results in unwanted feedrate fluctuation and further excited the vibration of the machine, although the curve itself is C^2-continuity. Some solutions are presented to decrease the fluctuation [20, 21], but it cannot be entirely eliminated. Clothoid curves, whose parameter describes its length, are always used as the transition between line and arc for the construction of high way or high-speed railway. In recent years, clothoid can also be seen for smoothing the CNC tool paths [22–24]. Since the traditional clothoid curves are defined in the plane, these solutions are only applied for the local smooth.

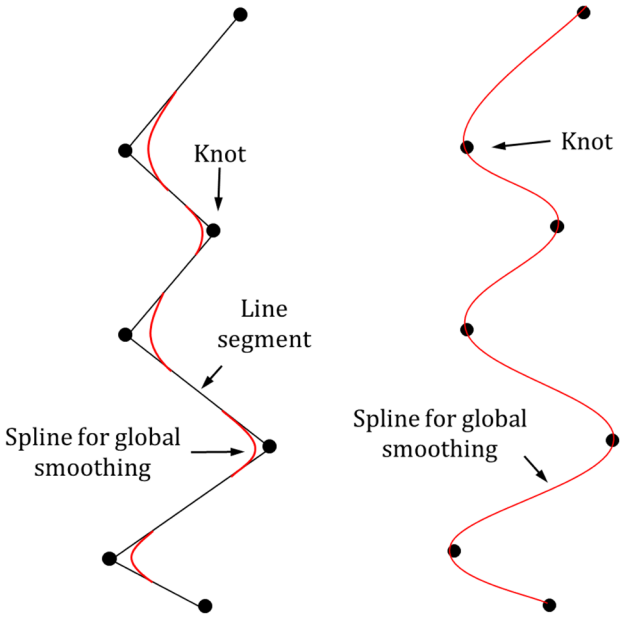

Fig. 2 Smooth strategy. Left: local; right: global

In this paper, the three-sectional 3D clothoid curve is proposed for the global fitting of the spatial curve. In order to satisfy the constraint of tool length, the TCP + TO representation is applied, where the orientation is globally smoothed through the B-spline with the desired order of continuity. Since the interpolation parameter of the 3D clothoid is the curve length, the feed fluctuation can be eliminated fundamentally. Compared with the state-of-the-art, the proposed solution decreases the feed fluctuation by more than one order of magnitude.

The remainder of this paper is organized as follows. After the short review, the three-sectional 3D clothoid curve is proposed in the Sect. 2. The tool orientation is smoothed and synchronized with the length of the TCP curve in the Sect. 3. In

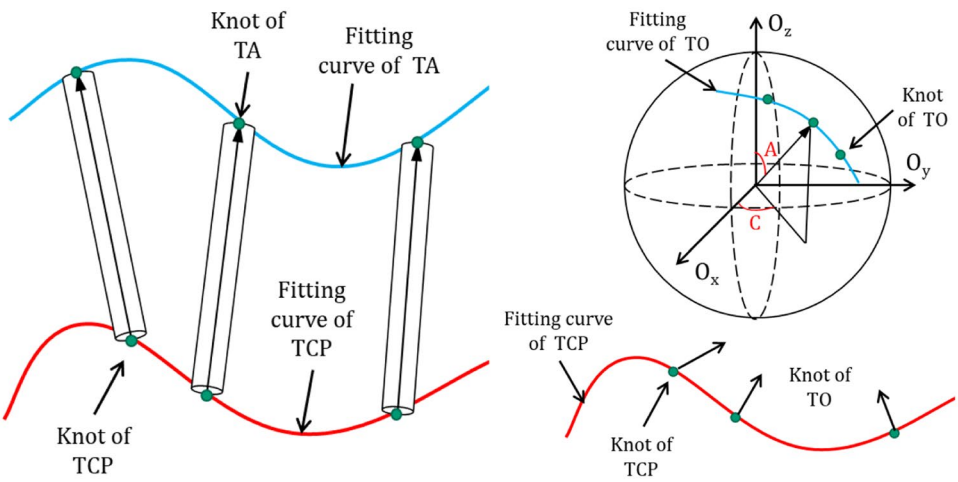

Fig. 1 Representation of tool pose. Left: TCP + TO; right: TCP + TA

the Sect. 4, the effectiveness of the proposed method is tested on and compared with the state-of-the-art. The Sect. 5 concludes the paper with comments.

2 Global smooth of TCP path through 3D clothoid

2.1 Definition of 3D clothoid

Supposing the 2D clothoid is defined on the *X*–*Y* plane, the 3D clothoid can be regarded as the extension of the 2D curve along the *Z* direction. As shown in Fig. 3, if the tangent vector of a curve can be described as

$$\vec{t} = \begin{pmatrix} t_x \\ t_y \\ t_z \end{pmatrix} = \begin{pmatrix} cos(\varphi(u))cos(\theta(u)) \\ cos(\varphi(u))sin(\theta(u)) \\ sin(\varphi(u)) \end{pmatrix} \tag{1}$$

the 3D clothoid can be formulated as

$$\vec{r}(u) = \vec{r}(u_0) + \int_{s_0}^{s} \vec{t}du = \begin{pmatrix} x_0 + \int_{s_0}^{s} \cos(\varphi(u))\cos(\theta(u))du \\ y_0 + \int_{s_0}^{s} \cos(\varphi(u))sin(\theta(u))du \\ z_0 + \int_{s_0}^{s} sin(\varphi(u))du \end{pmatrix} \tag{2}$$

where s is the length of the curve, $\varphi \in \left[-\pi/2 \ \pi/2\right]$ denotes the angle from the *X*–*Y* plane to the tangent vector, $\theta \in \left[0 \ 2\pi\right]$ denotes the angel from *X*-axis to the vector $\boldsymbol{t}_1$.

Property 1: The interpolation parameter u of the 3D clothoid is the length of the curve s.

Prove: In a narrow neighborhood, the length of the curve can be approximated as the length of the chord.

$$\begin{aligned} &\Delta s \approx \left|\vec{r}(u+\Delta u) - \vec{r}(u)\right| = \sqrt{\Delta x^2 + \Delta y^2 + \Delta z^2} \\ &\Rightarrow \lim_{\Delta u \to 0} \frac{\Delta s}{\Delta u} = \frac{ds}{du} = \sqrt{\left(\frac{dx}{du}\right)^2 + \left(\frac{dy}{du}\right)^2 + \left(\frac{dz}{du}\right)^2} \\ &\Rightarrow \frac{ds}{du} = \sqrt{t_x^2 + t_y^2 + t_z^2} = 1 \\ &\Rightarrow s = u + c \end{aligned} \tag{3}$$

where the constant c describes the offset between s and u depending on the initial position of the curve.

The derivative of the tangent vector is the curvature vector, which is calculated as follows.

$$\begin{aligned} &\frac{\vec{dt}}{ds} = \begin{pmatrix} -\varphi' sin\varphi cos\theta - \theta' cos\varphi sin\theta \\ -\varphi' sin\varphi sin\theta + \theta' cos\varphi cos\theta \\ \varphi' cos\varphi \end{pmatrix} = \vec{\kappa} \\ &\|\vec{\kappa}\| = \sqrt{\vec{\kappa}^T \cdot \vec{\kappa}} = \sqrt{\left(\frac{d\varphi}{ds}\right)^2 + \left(\frac{d\theta}{ds}\cos\varphi\right)^2} = \kappa \end{aligned} \tag{4}$$

The norm of the curvature vector is the curvature of the curve κ, and the normalized $\vec{\kappa}$ defines the direction of principle normal $\vec{\boldsymbol{n}} = \vec{\kappa}/||\vec{\kappa}||$. Since the $\vec{\kappa}$ is always defined in a plane orthogonal to $\vec{t}$, it has 2 degrees of freedom and can be defined on two different bases. Therefore, the curvature in this paper is determined with the "directions" of φ and θ.

$$\begin{aligned} \frac{d\varphi}{ds} &= \kappa_\varphi + \kappa'_\varphi s + \frac{1}{2}\kappa''_\varphi s^2 + \cdots = \sum_{i=0}^{n} \frac{s^i}{i!}\kappa_\varphi^{(i)} \\ \frac{d\theta}{ds} &= \kappa_\theta + \kappa'_\theta s + \frac{1}{2}\kappa''_\theta s^2 + \cdots = \sum_{i=0}^{n} \frac{s^i}{i!}\kappa_\theta^{(i)} \end{aligned} \tag{5}$$

where (i) means the ith-derivative, and their values will be determined by the global smoothing introduced in the next section. Through the integration of Eq. (5), the φ and θ can be formulated as follows:

$$\begin{aligned} \varphi &= \varphi_0 + \kappa_\varphi s + \frac{1}{2}\kappa'_\varphi s^2 + \cdots = \varphi_0 + \sum_{i=1}^{n} \frac{s^i}{i!}\kappa_\varphi^{(i-1)} \\ \theta &= \theta_0 + \kappa_\theta s + \frac{1}{2}\kappa'_\theta s^2 + \cdots = \theta_0 + \sum_{i=1}^{n} \frac{s^i}{i!}\kappa_\theta^{(i-1)} \end{aligned} \tag{6}$$

where φ_0 and θ_0 are the two initial angles corresponding to the starting point. The tangent vector is constructed to be the composition of the trigonometric function and the functions written as Eq. (6). Since the addition and the multiplication of *sin* and *cos* are infinitely derivable, the order of derivability, as well as the continuity, is dominated by n in Eq. (6).

2.2 Global smooth of TCP curve through three-sectional clothoid

Most curves applied in the industry require C^2-continuity, so in this section, we will mainly present the concept for global

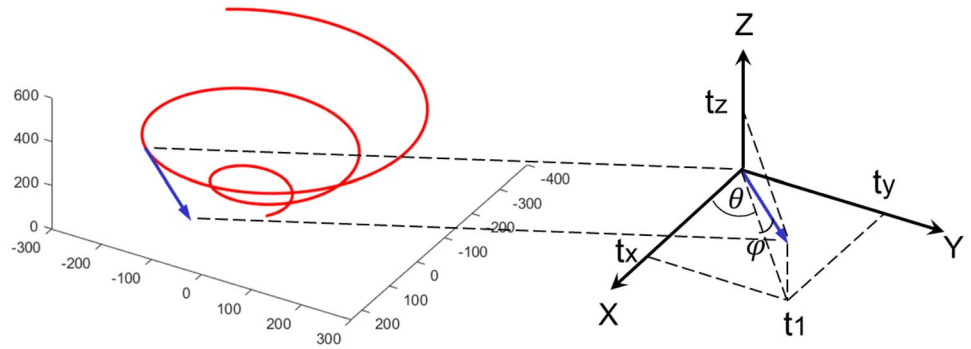

Fig. 3 3D clothoid and its tangent vector

smoothing with C^2-continuity. The presented method can also expand for the curve with a higher order of continuity.

The idea is to connect two neighboring knots with three C^2 clothoid curves described as follows.

$$\vec{r}(s)=\begin{pmatrix} x_{j-1}+\int_0^s \cos\left(\varphi_{j-1}+\kappa_{\varphi,j-1}s+\frac{1}{2}\kappa'_{\varphi,j}s^2\right)\cos\left(\theta_{j-1}+\kappa_{\theta,j-1}s+\frac{1}{2}\kappa'_{\theta,j}s^2\right)du \\ y_{j-1}+\int_0^s \cos\left(\varphi_{j-1}+\kappa_{\varphi,j-1}s+\frac{1}{2}\kappa'_{\varphi,j}s^2\right)sin\left(\theta_{j-1}+\kappa_{\theta,j-1}s+\frac{1}{2}\kappa'_{\theta,j}s^2\right)du \\ z_{j-1}+\int_0^s sin\left(\varphi_{j-1}+\kappa_{\varphi,j-1}s+\frac{1}{2}\kappa'_{\varphi,j}s^2\right)du \end{pmatrix} j=1,2,3 \tag{7}$$

where φ_1, φ_2 and θ_1, θ_2 are the tangent angles corresponding to the connecting points between the three clothoid curves. And φ_3 and θ_3 are the two tangent angles corresponding to the end of the third clothoid curve, whose values are given through the G-code.

Since these three curves are transited with C^2-continuity, the curvatures should be satisfied the following conditions.

$$\begin{cases} \kappa_{i,1}=\kappa_{i,0}+\kappa'_{i,1}S_1 \\ \kappa_{i,2}=\kappa_{i,1}+\kappa'_{i,2}S_2 \\ \kappa_{i,3}=\kappa_{i,2}+\kappa'_{i,3}S_3 \end{cases} i=\varphi,\theta \tag{8}$$

where S_1, S_2, S_3 are the lengths of three clothoid curves, respectively. $\kappa_{i,j}$ with $i=\varphi$, θ and $j=0, 1, 2$ is the curvature at the starting point of the three clothoid curves. The derivatives of curvatures are the parameters that need to be solved. The tangent of three clothoid segments should also be transited continuously,

$$\begin{cases} \varphi_1=\varphi_0+\kappa_{\varphi,0}S_1+\frac{1}{2}\kappa'_{\varphi,1}S_1 \\ \varphi_2=\varphi_1+\kappa_{\varphi,1}S_2+\frac{1}{2}\kappa'_{\varphi,2}S_2 \\ \varphi_3=\varphi_2+\kappa_{\varphi,2}S_3+\frac{1}{2}\kappa'_{\varphi,3}S_3 \\ \theta_1=\theta_0+\kappa_{\theta,0}S_1+\frac{1}{2}\kappa'_{\theta,1}S_1 \\ \theta_2=\theta_1+\kappa_{\theta,1}S_2+\frac{1}{2}\kappa'_{\theta,2}S_2 \\ \theta_3=\theta_2+\kappa_{\theta,2}S_3+\frac{1}{2}\kappa'_{\theta,3}S_3 \end{cases} \tag{9}$$

as well as the position.

$$\begin{cases} \vec{r}_1=\vec{r}_0+\vec{r}(S_1) \\ \vec{r}_2=\vec{r}_1+\vec{r}(S_2) \\ \vec{r}_3=\vec{r}_2+\vec{r}(S_3) \end{cases} \tag{10}$$

The coordinate of the knots $\vec{r}_0$ and $\vec{r}_3$ are given by the G-code. The tangent and the curvature should also be determined firstly as the premise of the smoothing. Similar to the quintic interpolation presented in [18, 21], the tangent and the curvature of the knots are determined through the Akima fitting, which fits the four neighboring knots with a 3-order polynomial; see Sect. 3.2. The curve tangent and curvature at each knot can be obtained through the derivatives of the Akima-polynomials.

If the normalized first- and second-order derivatives at knot k are $(\dot{x}_k\ \dot{y}_k\ \dot{z}_k)$ and $(\ddot{x}_k\ \ddot{y}_k\ \ddot{z}_k)$, the tangent angle and the components of curvature can be formulated as follows.

$$\theta_0\begin{cases} \varphi_0=\arcsin(\dot{z}_k) \\ \arccos\left(\frac{\dot{x}_k}{\cos\varphi_0}\right) & \dot{y}_k\geq 0 \\ 2\pi-\arccos\left(\frac{\dot{x}_k}{\cos\varphi_0}\right) & \dot{y}_k<0 \end{cases} \tag{11}$$

$$\theta_3\begin{cases} \varphi_3=\arcsin(\dot{z}_{k+1}) \\ \arccos\left(\frac{\dot{x}_{k+1}}{\cos\varphi_3}\right) & \dot{y}_{k+1}\geq 0 \\ 2\pi-\arccos\left(\frac{\dot{x}_{k+1}}{\cos\varphi_3}\right) & \dot{y}_{k+1}<0 \end{cases} \tag{12}$$

$$\kappa_{\theta,0}\begin{cases} \kappa_{\varphi 0}=\frac{\ddot{z}_k}{\cos\varphi_0} \\ \frac{\sin\varphi_0\cos\theta_0\kappa_{\varphi,0}-\ddot{x}_k}{\cos\varphi_0\sin\theta_0} & \sin\theta_0\neq 0 \\ \frac{\ddot{x}_k}{\cos\varphi_0\cos\theta_0} & \sin\theta_0=0 \end{cases} \tag{13}$$

$$\begin{cases} \kappa_{\varphi,3}=\frac{\ddot{z}_{k+1}}{\cos\varphi_3} \\ \frac{\sin\varphi_3\cos\theta_3\kappa_{\varphi,3}-\ddot{x}_{k+1}}{\cos\varphi_3\sin\theta_3} & \sin\theta_3\neq 0 \\ \frac{\ddot{x}_{k+1}}{\cos\varphi_3\cos\theta_3} & \sin\theta_3=0 \end{cases} \tag{14}$$

When the position, tangent, and curvature vectors are well determined, the following constraints according to the C^2/C^1/C^0 continuities can be listed.

$$\begin{aligned} \kappa_{\varphi,3}&=\kappa_{\varphi,0}+\sum_{j=1}^3\kappa'_{\varphi,j}S_j \\ \kappa_{\theta,3}&=\kappa_{\theta,0}+\sum_{j=1}^3\kappa'_{\theta,j}S_j \\ \varphi_3&=\varphi_0+\sum_{j=1}^3\left(\kappa_{\theta,j}S_j+\frac{1}{2}\kappa'_{\theta,j}S_j^2\right) \\ \theta_3&=\theta_0+\sum_{j=1}^3\left(\kappa_{\theta,j}S_j+\frac{1}{2}\kappa'_{\theta,j}S_j^2\right) \\ x_{k+1}&=x_k+\sum_{j=1}^3\int_0^{S_j}\cos\varphi(u)\cos\theta(u)du \\ y_{k+1}&=y_k+\sum_{j=1}^3\int_0^{S_j}\cos\varphi(u)sin\theta(u)du \\ z_{k+1}&=z_k+\sum_{j=1}^3\int_0^{S_j}sin\varphi(u)du \end{aligned} \tag{15}$$

In Eq. (15), there are 9 parameters to be determined. They are S_j and $\kappa'_{i,j}$ with $i=\varphi$, θ and $j=1, 2, 3$. However, there are only 7 constraints in Eq. (15). To solve the parameters, two additional constraints are considered, $S_1=S_2=S_3$. These two constraints simplify the

procedure of computation and avoid the ill-solution with a negative value of S.

3 Tool path smoothing for 5-axis machining

The TCP + TO representation is used in this paper, so in this section, the global smoothing method of tool orientation with B-spline is introduced firstly, and then the curve parameter of TO is synchronized with the curve length of TCP.

3.1 Global smoothing of tool orientation

The tool orientations given by the CAM are normally denoted with the A and C angle, which presents the rotation around the X and Z axis in the workpiece coordinate system, respectively. However, such representation may lead to singularity, when the orientation swings through the direction of the Z-axis. Therefore, in this paper, the tool orientation is presented through a normalized vector $\vec{o} = \begin{bmatrix} o_x & o_y & o_z \end{bmatrix}^T$ with

$$\begin{aligned} o_x &= cos\ A cos\ C \\ o_y &= cos\ A\ sin\ C \\ o_z &= sin\ A \end{aligned} \tag{16}$$

The method for fitting the TO with B-spline is depicted in Fig. 4.

Generally, a B-spline can be constructed as follow.

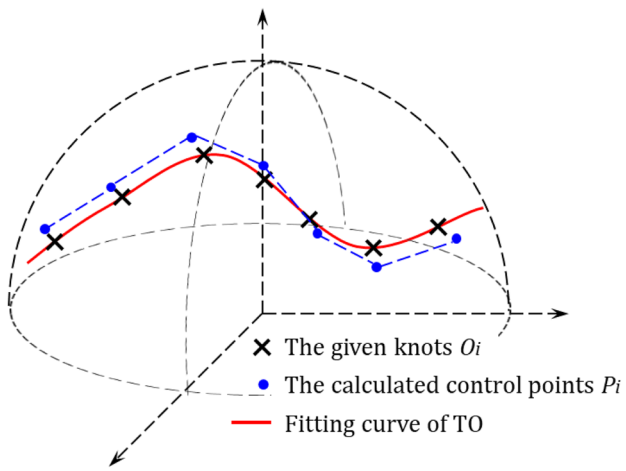

Fig. 4 Global smoothing of tool orientation through B-spline

$$\vec{o}(u) = \sum_{i=0}^{n} N_{i,r}(u) P_i \tag{17}$$

where P is the control point, and N is the basic function derived through the Cox–de Boor recursion formula.

$$\begin{aligned} N_{i,r}(u) &= \frac{u-u_i}{u_{i+r}-u_i} N_{i,r-1}(u) + \frac{u_{i+r+1}-u}{u_{i+r+1}-u_{i+1}} N_{i+1,r-1}(u) \\ N_{i,0}(u) &= \begin{cases} 1 & u_i \le u < u_{i+1} \\ 0 & otherwise \end{cases} \end{aligned} \tag{18}$$

with r is the degree of the spline.

The orientation O given by the CAM cannot be directly used as the control point, since the B-spline with a high order of continuity does not pass through its control points. Supposing there are some certain parameters $\overline{u}_i$, with which the fitting curve just passes through the given orientation O_i,

$$\underbrace{\begin{bmatrix} N_{0,r}(\overline{u}_0) & \cdots & N_{n,r}(\overline{u}_0) \\ \vdots & \ddots & \vdots \\ N_{0,r}(\overline{u}_n) & \cdots & N_{n,r}(\overline{u}_n) \end{bmatrix}}_{\Phi} \underbrace{\begin{bmatrix} P_0 \\ \vdots \\ P_n \end{bmatrix}}_{\Gamma} = \underbrace{\begin{bmatrix} O_0 \\ \vdots \\ O_n \end{bmatrix}}_{\Psi} \tag{19}$$

the control points can be solved as follows.

$$\Gamma = \Phi^{-1} \Psi \tag{20}$$

To solve Eq. (20), the parameters $\overline{u}_i$, as well as the elements u_i of the knot vector, should be defined firstly. The $\overline{u}_i$ is determined based on the method of chord length parameterization. Since the B-spline is used for fitting the TO, the angle between two neighboring orientations is regarded as the chord length for the computation. The total chord length can be calculated as follows:

$$\Omega = \sum_{i=1}^{n} \left| \arccos\left(O_{i-1} \cdot O_i \right) \right| \tag{21}$$

so that the $\overline{u}_i$ can be normalized under the following definition.

$$\overline{u}_i = \overline{u}_{i-1} + \frac{\left| \arccos\left(O_{i-1} \cdot O_i \right) \right|}{\Omega}, \quad i = 1, 2, \cdots, n \tag{22}$$

The clamped knot vector is applied here. If the number of control points is $n+1$, there are totally $n+r+1$ elements in the knot vector. The first $r+1$ elements equal 0, the last $r+1$ elements equal 1, and the remainder of internal knots can be calculated as follows.

$$u_{k+r+1} = \frac{1}{r+1} \sum_{i=k}^{k+r} \overline{u}_i, k = 1, 2, \cdots, n-r-1 \tag{23}$$

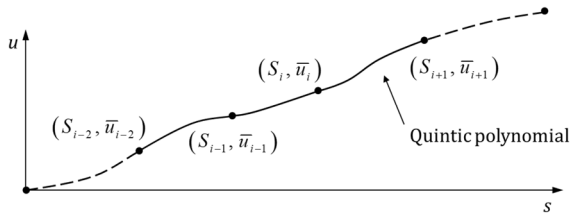

Fig. 5 Synchronizing TCP and TO through quintic polynomial

With such a defined knot vector, the curve can reach the first and the last control points. Furthermore, the matrix Φ will be simplified as a band matrix, so that the computing efficiency of the matrix inversion can be increased.

3.2 Synchronization of TCP and TO curves

The TCP and the TO are globally smoothed through their respective concept. To synchronize the rotation of the tool axis and the translation of the TCP, the curve parameter u of the B-spline should be related to the curve length s of the clothoid; see Fig. 5.

The quintic polynomial is applied to describe this relationship as follows.

$$u = A_i s^5 + B_i s^4 + C_i s^3 + D_i s^2 + E_i s + F_i s \in \left[0 \;\; L_{i,i+1}\right] \tag{24}$$

where $L_{i,i+1}$ denotes the curve length of the i-th segment from S_i to S_{i+1}. In Eq. (24), u is defined as a function of s, since the moving length of TCP at each sampling time is determined by the module of feedrate scheduling.

To solve the six polynomial coefficients in Eq. (24), the first and second derivatives at each end S_i and S_{i+1} should be determined through the Akima fitting firstly. Here, we also call the endpoint S_i or S_{i+1} as the knot, which is related to the points given by the CAM system; see Fig. 2. Take the calculation at S_i, for example, the Akima fitting can be mathematically described as follows.

$$u = G_i s^3 + H_i s^2 + J_i s + K_i \tag{25}$$

Different from the quintic spline, the Akima fitting is operated on the four neighboring knots S_{i-2}, S_{i-1}, S_i, and S_{i+1}. The curve lengths from S_{i-2} to S_{i-1}, S_i and S_{i+1} are denoted as $L_{i-2,i-1}$, $L_{i-2,i}$, and $L_{i-2,i+1}$, respectively. The position condition at four knots must be met for the Akima fitting.

$$\begin{aligned}
\bar{u}_{i-2} &= K_i \\
\bar{u}_{i-1} &= G_i L_{i-2,i-1}^3 + H_i L_{i-2,i-1}^2 + J_i L_{i-2,i-1} + K_i \\
\bar{u}_i &= G_i L_{i-2,i}^3 + H_i L_{i-2,i}^2 + J_i L_{i-2,i} + K_i \\
\bar{u}_{i+1} &= G_i L_{i-2,i+1}^3 + H_i L_{i-2,i+1}^2 + J_i L_{i-2,i+1} + K_i
\end{aligned} \tag{26}$$

where for each knot, the value of $\bar{u}_i$ is determined by Eq. (22). Therefore, the coefficients can be calculated as

$$\begin{bmatrix} G_i \\ H_i \\ J_i \end{bmatrix} = \begin{bmatrix} L_{i-2,i-1}^3 & L_{i-2,i-1}^2 & L_{i-2,i-1} \\ L_{i-2,i}^3 & L_{i-2,i}^2 & L_{i-2,i} \\ L_{i-2,i+1}^3 & L_{i-2,i+1}^2 & L_{i-2,i+1} \end{bmatrix}^{-1} \begin{bmatrix} \bar{u}_{i-1} - \bar{u}_{i-2} \\ \bar{u}_i - \bar{u}_{i-2} \\ \bar{u}_{i+1} - \bar{u}_{i-2} \end{bmatrix} \tag{27}$$

So that the first and second derivatives at S_i can be obtained as

$$\begin{aligned}
\bar{u}'_i &= 3G_i L_{i-2,i}^2 + 2H_i L_{i-2,i} + J_i \\
\bar{u}''_i &= 6G_i L_{i-2,i} + 2H_i
\end{aligned} \tag{28}$$

On the other hand, the quantic polynomial can also be derivated twice and set the derivative conditions with the value from Eq. (28).

$$\begin{aligned}
\bar{u}'_i &= u'(0) = E_i \\
\bar{u}''_i &= u''(0) = D_i \\
\bar{u}'_{i+1} &= u'\left(L_{i,i+1}\right) = 5A_i L_{i,i+1}^4 + 4B_i L_{i,i+1}^3 + 3C_i L_{i,i+1}^2 + 2U''_i L_{i,i+1} + U'_i \\
\bar{u}''_{i+1} &= u''\left(L_{i,i+1}\right) = 20A_i L_{i,i+1}^3 + 12B_i L_{i,i+1}^2 + 6C_i L_{i,i+1} + 2U''_i
\end{aligned} \tag{29}$$

With the position condition $U_i = u(0) = F_i$, the remaining parameters can be solved as follows.

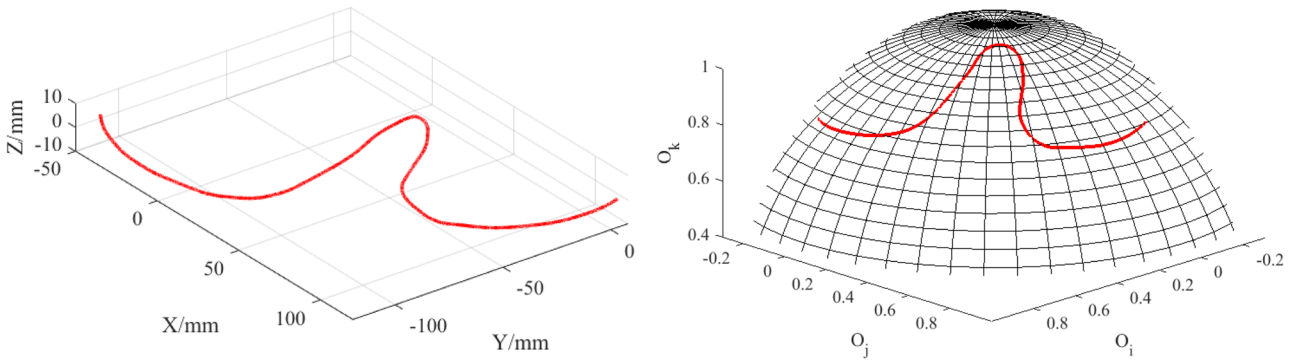

Fig. 6 The example tool path for the verification. Left: TCP path; right: TO path

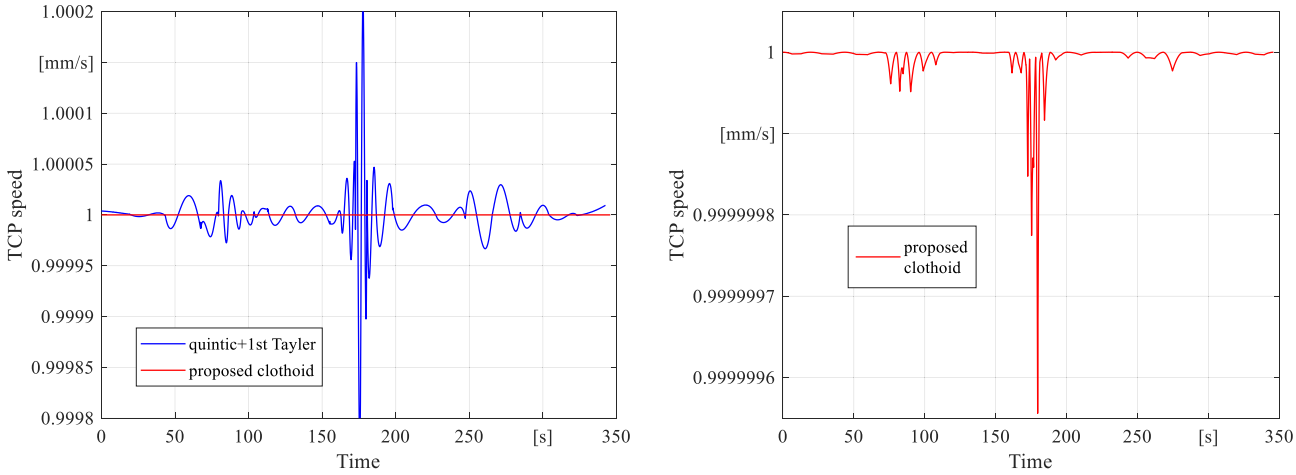

Fig. 7 Speed fluctuation of TCP. Left: comparison with state-of-the-art; right: presented method

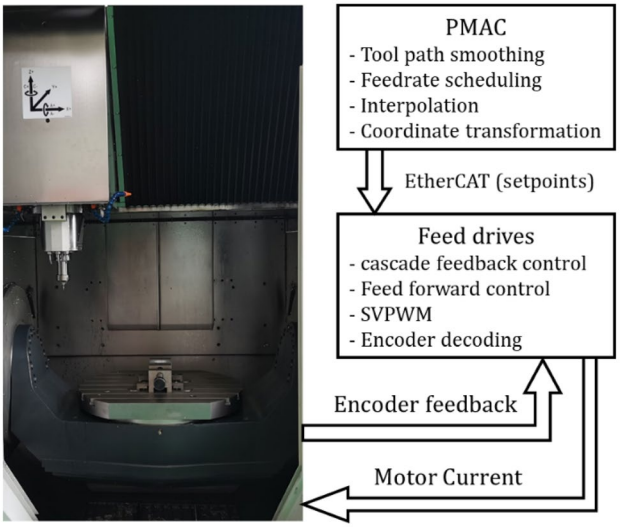

Fig. 8 The5-axis machine tool for experimental verification

$$\begin{bmatrix} A_i \\ B_i \\ C_i \end{bmatrix} = \begin{bmatrix} L^5_{i,i+1} & L^4_{i,i+1} & L^3_{i,i+1} \\ 5L^4_{i,i+1} & 4L^3_{i,i+1} & 3L^4_{i,i+1} \\ 20L^3_{i,i+1} & 12L^2_{i,i+1} & 6L_{i,i+1} \end{bmatrix}^{-1} \begin{bmatrix} \overline{u}_{i+1} - \overline{u}_i \\ \overline{u}'_{i+1} - \overline{u}'_i \\ \overline{u}''_{i+1} - \overline{u}''_i \end{bmatrix} \tag{30}$$

Through the quantic polynomial, the established relationship between u and s has a C^5-continuity in the segment and a C^2-continuity at each knot.

4 Verification of the proposed algorithm

Both simulative and experimental verifications were carried out to verify the effectiveness of the proposed smoothing concept. The data of the tool path used for the test is published in [14]. The paths of TCP and TO are plotted in Fig. 6.

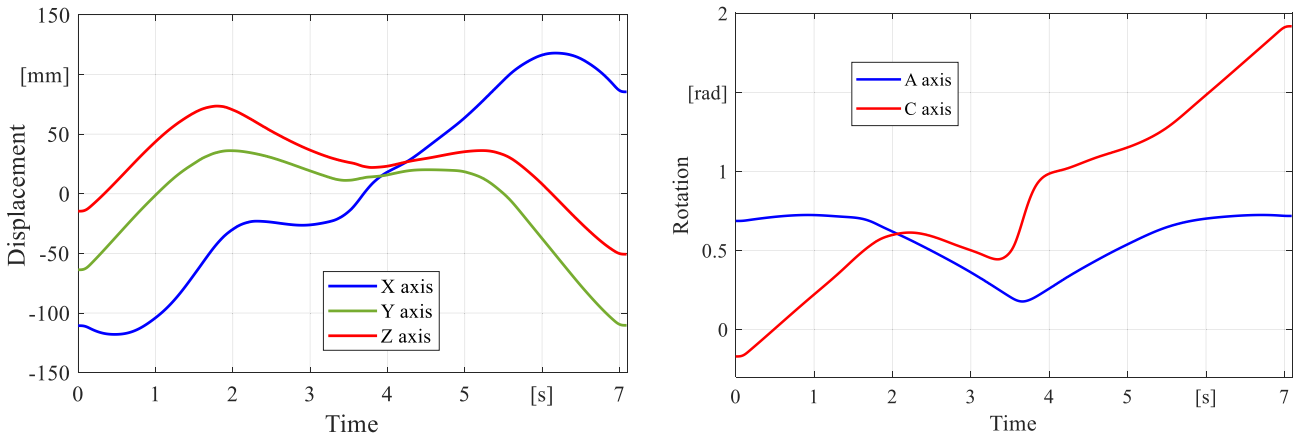

Fig. 9 Displacement of each axis. Left: X/Y/Z axes; right: A/C axes

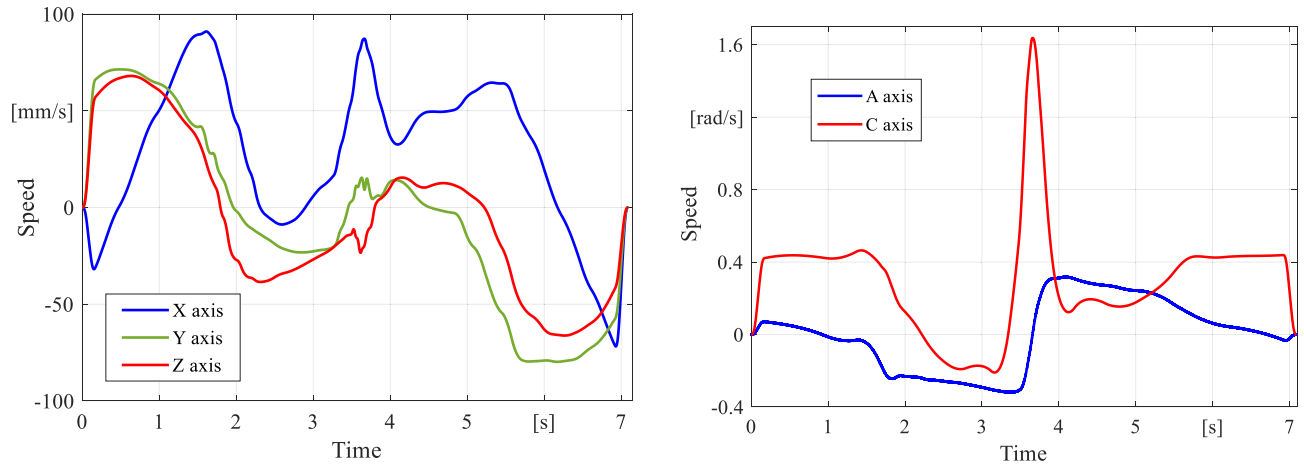

Fig. 10 Speed of each axis. Left: X/Y/Z axes; right: A/C axes

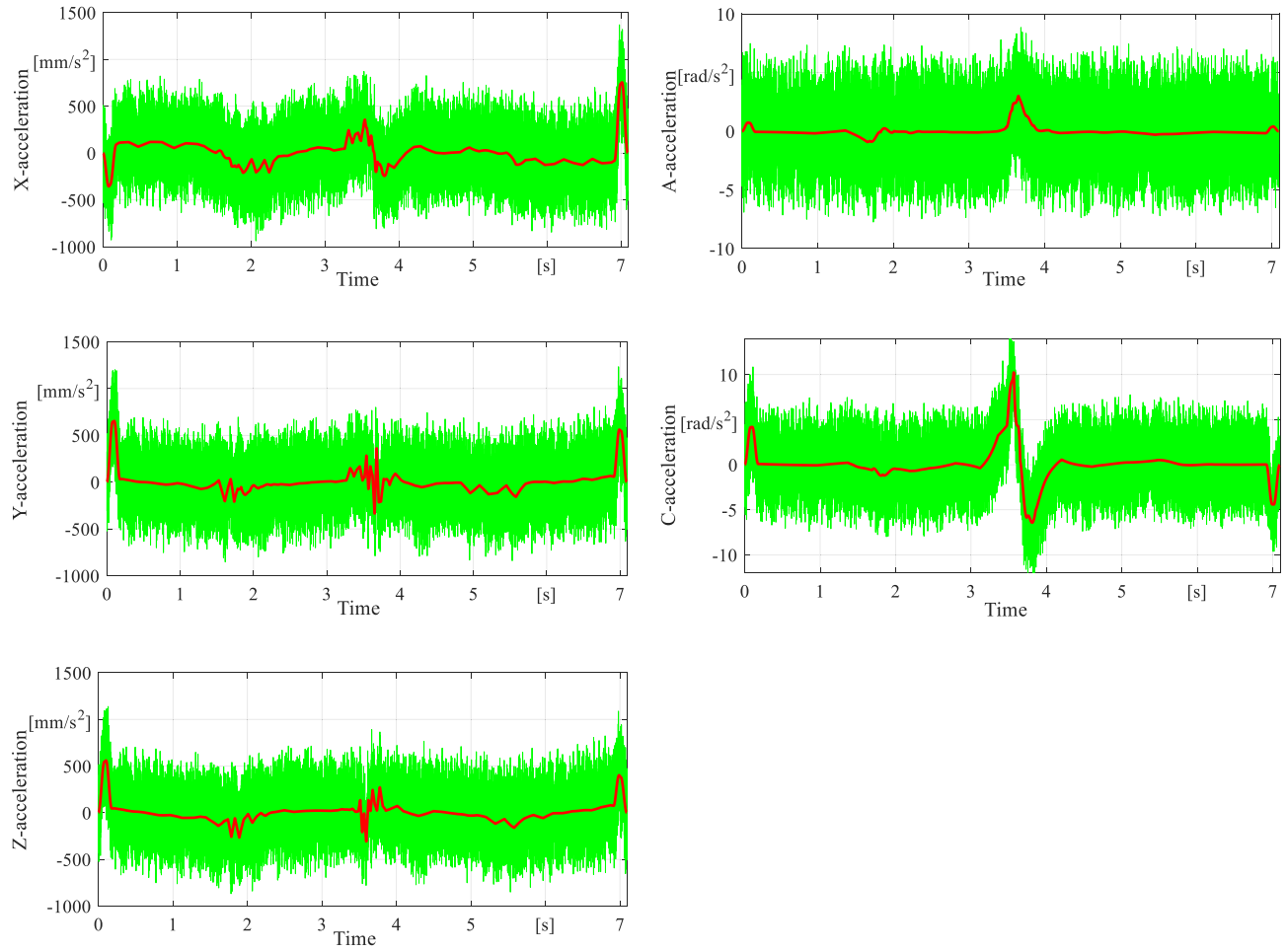

Fig. 11 Acceleration of each axis. Green: derived from the measured positions; red: derived from the reference positions

4.1 Simulative verification

For the simulative verification, the speed of TCP was set with the value of 1 mm/s and the interpolation frequency was set to be 100 Hz. Besides the proposed 3D clothoid interpolation method, the tool path was also interpolated through the quintic spline [18] with the 1st Tayler method [20] to decrease the speed fluctuation. The comparison for both methods is shown in Fig. 7.

The speed in Fig. 7 is calculated through the differencing of the interpolated displacement at each sampling time. It can be seen that the presented method attenuates the speed fluctuation over three orders of magnitude. The right subplot of Fig. 7 presents the fluctuation details of the clothoid interpolation. Because the clothoid curve is used to fit TCP, there is no nonlinear relationship between the interpolation parameters and the curve length, so the speed fluctuation of the tool is greatly reduced. The fluctuation is mainly caused by the truncation error of the clothoid at some places with large curvature.

4.2 Experimental verification

In Fig. 6, the presented tool path was also used for the experimental verification on a five-axis CNC machine (KMC600SU) with a tilting rotary table, as seen in Fig. 8. The offset between the A-axis and the origin of the workpiece coordinate system $L_{ac,z}=90$ mm.

The machine is controlled by a PMAC-system, where the proposed interpolation scheme is implemented. The tool path is smoothed and interpolated with a sampling frequency of 2 kHz. The interpolated setpoints are delivered through the EtherCAT to the feed drives of each axis, where the current (16 kHz), speed (4 kHz), and position control (2 kHz) loops with the feed-forward branch are operating in real-time.

This path is motion planed with a constant feedrate of 50 mm/s and the maximal acceleration and jerk of 500 mm/s^2 and 10,000 mm/s^3, respectively. The machine was operated without workpiece and cutting since the purpose of this experiment is to verify whether the

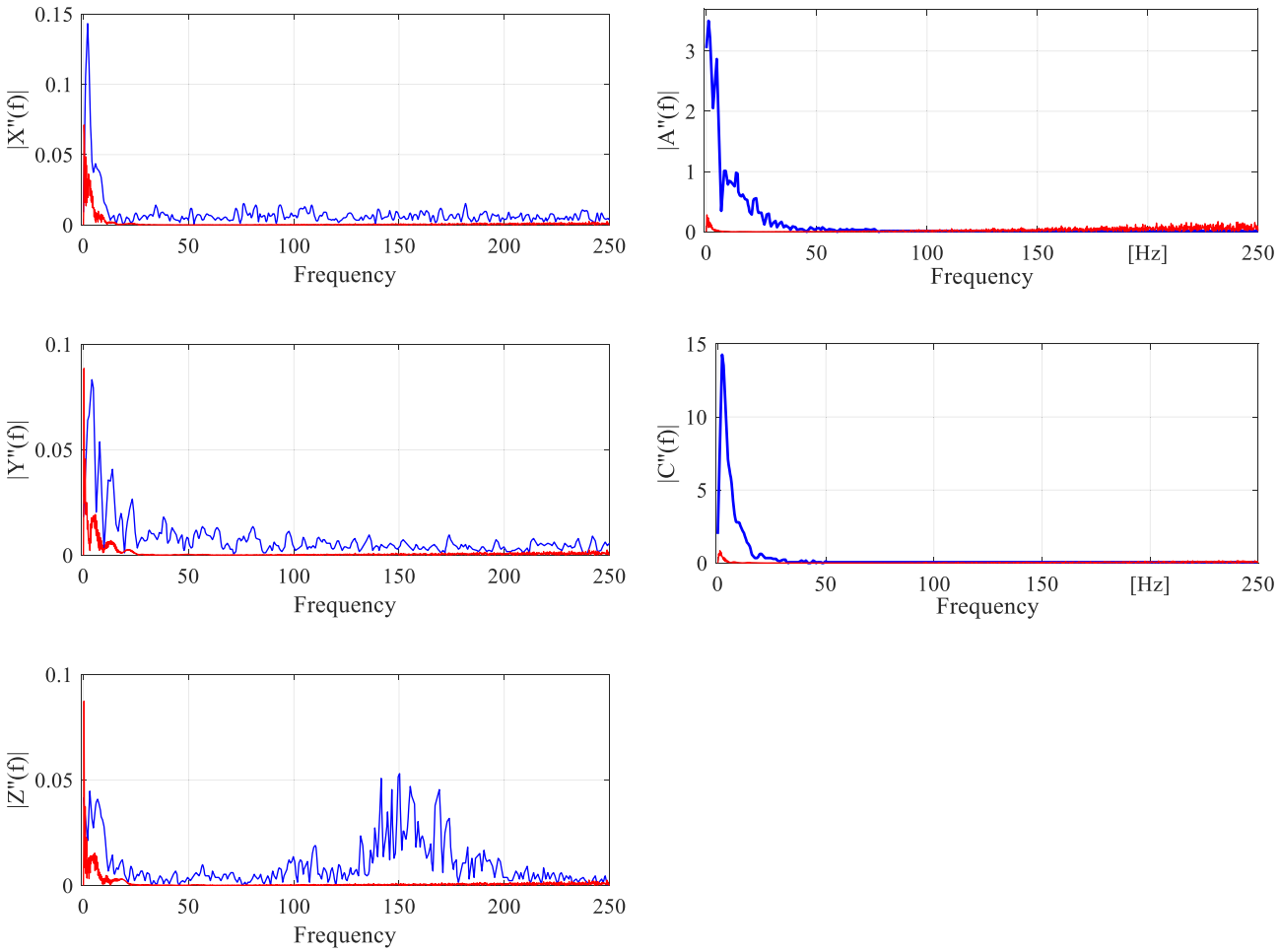

Fig. 12 Power spectrums from the FFT of the measured acceleration at each axis. Blue: C.^{3}-method presented in [15]; red: proposed method

proposed solution can attenuate the feed fluctuation or not when the setpoints are interpolated. The movements of each axis are gathered by the encodes and presented in Fig. 9.

The velocity and acceleration can be obtained through the differencing of position and are plotted in Figs. 10 and 11, respectively. Since the measurement noise will be extremely increased after differencing twice, the accelerations derived from the reference positions are also plotted in Fig. 11.

The effectiveness of the presented interpolation method can also be seen in the frequency domain. Figure 12 shows the acceleration power spectrums of each axis. For the comparison, the spectrums of the C^3-solution from [15], which also used the data from [14] for the experiment, are also plotted in Fig. 12. In [15], the paths of TCP and TO are global smoothed through B-spline with C^3-continuity separately and synchronized through a Bézier spline with 7-order. The length of the TCP curve is computed through the Simpson method and related to the interpolation parameter with a 9-order polynomial.

It can be observed that for the rotational axes, the power spectrum of the presented C^2-method is one order of magnitude lower than the C^3-method. For the translational axes, the spectrums are in the same order of magnitude near 0 Hz compared with the C^3-method but decay dramatically in the high-frequency range, which means less excitation on the machine structure.

5 Conclusion

This paper presented a global smoothing method for 5-axis interpolation. The path of the tool center point is fitting through the 3D clothoid. The path of the tool orientation is fitting in the spherical coordinate system through the B-spline with the required order. The TCP and TO are related by the quintic polynomial. Since the interpolation parameter of the clothoid curve is just the curve length, the presented method can theoretically eliminate all the feedrate fluctuation in the workpiece coordinate system, which is of great significance in the improvement of the machined surface quality. In the machine coordinate system, the proposed method presents a lower power spectrum of acceleration in the high-frequency range than the state-of-the-art, which is also meaningful for reducing the excitation of the machine structure.

Although the order of curve continuity does have an impact on the feed fluctuation at each machine axis, the dominant factor for the fluctuation is the nonlinearity between the interpolation parameter u and the curve length s. Therefore, we believe that the effective way to attenuate the feed fluctuation is to find out the solvable relationship between u and s, not the unconditional increasing the order of continuity of the tool path.

Author contribution Zheng Sun: methodology, writing, funding acquisition; Liyong Niu: software, formal analysis; Bin Liu: validation, funding acquisition; Kedian Wang: project administration; Bo Li: validation; Xuesong Mei: conceptualization, supervision.

Funding This research is financially supported by the National Natural Science Foundation of China under grant 51975461, the Natural Science Foundation of Jiangsu Province under No. BK20190217, and the Department of Science and Technology of Shaanxi Province under grant 2019ZDLGY14-07.

Declarations

Ethics approval Not applicable.

Consent to participate Not applicable.

Consent for publication Not applicable.

Competing interests The authors declare no competing interests.

References

1. Beudaert X, Lavernhe S, Toumier C (2013) 5-axis local corner rounding of linear tool path discontinuities. Int J Mach Tools Manuf 73:9–16. https://doi.org/10.1016/j.ijmachtools.2013.05.008
2. Xu F, Sun Y (2018) A circumscribed corner rounding method based on double cubic B-splines for a five-axis linear tool path. The International Journal of Advanced Manufacturing Technology 94:451–462. https://doi.org/10.1007/s00170-017-0869-x
3. Zhang L, Zhang K, Yan Y (2016) Local corner smoothing transition algorithm based on double cubic nurbs for five-axis linear tool path. Journal of Mechanical Engineering 62(11):647–656. https://doi.org/10.5545/sv-jme.2016.3525
4. Jin Y, Bi Q, Wang Y (2015) Dual-Bezier path smoothing and interpolation for five-axis linear tool path in workpiece coordinate system. Adv Mech Eng 7(7):1–14. https://doi.org/10.1177/1687814015595211
5. Fan W, Ji J, Wu P, Wu D, Chen H (2019) Modeling and simulation of trajectory smoothing and feedrate scheduling for vibration-damping CNC machining. Simul Model Pract Theory 99:102028. https://doi.org/10.1016/j.simpat.2019.102028
6. Tulsyan S, Altintas Y (2015) Local toolpath smoothing for five-axis machine tools. Int J Mach Tools Manuf 96:15–26. https://doi.org/10.1016/j.ijmachtools.2015.04.014
7. Yang J, Yuen A (2017) An analytical local corner smoothing algorithm for five-axis CNC machining. Int J Mach Tools Manuf 123:22–35. https://doi.org/10.1016/j.ijmachtools.2017.07.007
8. Shi J, Bi Q, Wang Y (2015) Corner rounding of linear five-axis tool path by dual PH curves blending. Int J Mach Tools Manuf 88:223–236. https://doi.org/10.1016/j.ijmachtools.2014.09.007
9. Li Y, Wang Y, Feng J, Yang J (2008) The research of dual NURBS curves interpolation algorithm for high-speed five-axis machining. In: Xiong C., Proceedings of Intelligent Robotics and Applications: 983–992. https://doi.org/10.1007/978-3-540-88518-4_105
10. Bi Q, Wang Y, Zhu L, Ding H (2010) An algorithm to generate compact dual NURBS tool path with equal distance for 5-axis NC machining Proceedings of International Conference on Intelligent Robotics and Applications 553–564. https://doi.org/10.1007/978-3-642-16587-0_51

11. Zhang J, Zhang L, Zhang K, Mao J (2016) Double NURBS trajectory generation and synchronous interpolation for five-axis machining based on dual quaternion algorithm. The International Journal of Advanced Manufacturing Technology 83:2015–2025. https://doi.org/10.1007/s00170-015-7723-9
12. Langeron J, Duc E, Lartigue C, Bourdet P (2004) A new format for 5-axis tool path computation, using Bspline curves. Comput Aided Des 36(12):1219–1229. https://doi.org/10.1016/j.cad.2003.12.002
13. Wang X, Liu B, Mei X, Hou D, Li Q, Sun Z (2021) Global smoothing for five-axis linear paths based on an adaptive NURBS interpolation algorithm. Int J Adv Manuf Technol 114:2407–2420. https://doi.org/10.1007/s00170-021-07013-6
14. Fleisig R, Spence A (2001) A constant feed and reduced angular acceleration interpolation algorithm for multi-axis machining. Comput Aided Des 33(1):1–15. https://doi.org/10.1016/S0010-4485(00)00049-X
15. Yuen A, Zhang K, Altintas Y (2013) Smooth trajectory generation for five-axis machine tools. Int J Mach Tools Manuf 71:11–19. https://doi.org/10.1016/j.ijmachtools.2013.04.002
16. Gao X, Zhang S, Qiu L, Liu X, Wang Z, Wang Y (2020) Double B-spline curve-fitting and synchronization-integrated feedrate scheduling method for five-axis linear-segment toolpath. Appl Sci 10(9):3158. https://doi.org/10.3390/app10093158
17. Li D, Zhang W, Zhou W, Shang T, Fleischer J (2018) Dual NURBS path smoothing for 5-axis linear path of flank milling. Int J Precis Eng Manuf 19:1811–1820. https://doi.org/10.1007/s12541-018-0209-6
18. Wang DC, Yang DCH (1993) Nearly arc-length parameterized quintic-spline interpolation for precision machining. Comput Aided Des 25(5):281–288. https://doi.org/10.1016/0010-4485(93)90085-3
19. Farouki R, Shah S (1996) Real-time CNC interpolators for Pythagorean-hodograph curves. Computer Aided Geometric Design 13(7):583–600. https://doi.org/10.1016/0167-8396(95)00047-X
20. Shpitalni M, Koren Y, Lo C-C (1994) Realtime curve interpolators. Comput Aided Des 26(11):832–838. https://doi.org/10.1016/0010-4485(94)90097-3
21. Erkorkmaz K, Altintas Y (2005) Quintic spline interpolation with minimal feed fluctuation. J Manuf Sci Eng 127(2):339–349. https://doi.org/10.1115/1.1830493
22. Dripke C, Groh F, Keinert M, Verl A (2014) A new approach to interpolation of tool path trajectories with piecewise defined clothoids. Enabling Manufacturing Competitiveness and Economic Sustainability 249–254. https://doi.org/10.1007/978-3-319-02054-9_42
23. Atmosudiro A, Verl A, Lechler A, Schwarz G (2017) Evaluation of clothoids in manufacturing context. Procedia CIRP 62:541–546. https://doi.org/10.1016/j.procir.2016.06.066
24. Huang X, Zhao F, Tao T, Mei X (2020) A novel local smoothing method for five-axis machining with time-synchronization feedrate scheduling. IEEE Access 8:19659463. https://doi.org/10.1109/ACCESS.2020.2992022